Reversible Switching between Hydrophilic and Hydrophobic Superparamagnetic Iron Oxide Microspheres via One-Step Supramolecular Dynamic Dendronization: Exploration of Dynamic Wettability

Ken Cham-Fai Leung,* Shouhu Xuan, and Chui-Man Lo

Center of Novel Functional Molecules, Department of Chemistry, The Chinese University of Hong Kong, Shatin, NT, Hong Kong SAR

ABSTRACT We describe the use of hydrophobic poly(aryl ether) dendrons to peripherally functionalize hydrophilic amine-containing superparamagnetic iron oxide microspheres (**SPIO-NH₂**) in one step via imine formation. The reversible formation of imine bonds in the absence/presence of water renders dynamic control of the hydrophilicity and hydrophobicity of the microspheres (**SPIO-Gn**). The dynamic nature of the imine-containing dendronized microspheres (**SPIO-Gn**) can be "fixed" by locking the reversible 2,6-diiminopyridyl moieties with metal cations (Zn^{2+}, Co^{2+}, and Ni^{2+}) to afford kinetically stable dendronized microspheres (**SPIO-Gn-M**). Isolation of these microspheres is facilitated by convenient magnetic separation by an externally applied magnetic field. Characterization of these novel organic—inorganic hybrid microspheres has been performed by various techniques using UV/visible absorption and Fourier transform infrared spectroscopies, transmission electron microscopy, thermogravimetric analysis, and a vibrating sample magnetometer. We have demonstrated the stability and reversible switching of hydrophilicity/hydrophobicity by contact-angle measurements. In particular, the hydrophilic **SPIO-NH₂** microspheres demonstrated a contact angle of $42 \pm 2°$ when a drop of water was added to a **SPIO-NH₂**-coated mica surface. On the other hand, the hydrophobic **SPIO-Gn-M** dendronized microspheres demonstrated a contact angle of $85 \pm 2°$, an observation that involves an increase of the contact angle of over 40°. Furthermore, when a drop of water was placed on a dynamic **SPIO-Gn**-coated mica surface, the contact angle of the water droplet decreased in time. Comparatively, the rate of decrease of the contact angle is H_2O > 1 % $Co(OAc)_2/H_2O$ > N,N'-dimethylformamide/H_2O (1:1).

KEYWORDS: dendrimer • dynamic covalent chemistry • hydrophobic • imine • iron oxide

INTRODUCTION

Recently, the preparation of organic—inorganic hybrid materials that utilizes various supramolecular driving forces has been progressing rapidly (1). In particular, organic molecular or nanoscale materials that are tethered on solid supports such as spherical particles, thin solid films, or metal surfaces form self-assembling monolayers with specific functions. Moreover, stimuli-responsive supramolecular recognition motifs could be utilized and easily manipulated for reversible control of the molecular motions, size, and subsequent intrinsic properties (2). Reversible control between hydrophilic and hydrophobic surfaces offers considerable applications in surface science and microfluidic systems (3). Nature uses specific molecular motors and machines to create rational controlled movements and functions. The research on mimicking these molecular machines has recently gained a lot of attention. In particular, Leigh et al. (3a) reported that a surface that was coated with bistable rotaxane molecules possesses remarkable macro-scopic transport of liquids. Furthermore, Meijer et al. (3b) reported the controlled directional movement of amine-rich dendrimers on aldehyde-functionalized gradient surfaces by virtue of reversible imine formation.

The research of superparamagnetic iron oxide (SPIO)-based composite nanomaterials is getting mature because it offers the possibility to create new generations of nano-structured materials with diverse applications for unique magnetic responsivity, low cytotoxicity, and chemically functionable surface. Areas of application of iron oxide particles that are coated with silica, dextran, etc., include magnetic resonance imaging (MRI) contrast agents, separation and purification of biomolecules, magnetic-targeted drug delivery, and catalyst supports (4).

On the other hand, supramolecular complexation between Schiff bases (imines) (5) and metal cations represents a versatile way to construct sophisticated molecular structures such as Borromean rings (6), Solomon knots (7), molecular capsules (8), etc. The formation of imine bonds requires a reversible condensation between amines and carbonyl/aldehyde groups. The imine bond is regarded as one of the dynamic covalent bonds (9) based on the fact that they are susceptible in hydrolysis and imine exchange.
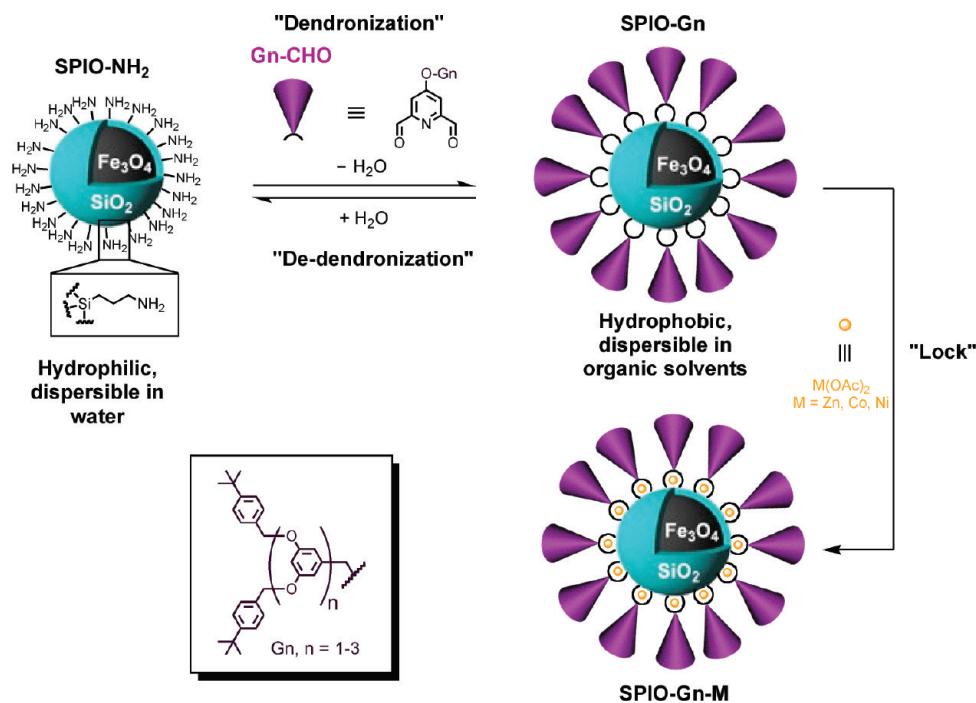
Scheme 1. Graphical Representation of the Reversible Control between Hydrophilic SPIO-NH$_2$ Microspheres and Hydrophobic Dendronized SPIO-G*n* Microspheres in the Absence/Presence of Water^a

^{a} The dynamic dendronized **SPIO-G*n*** microspheres can be locked by metal templation to give kinetically stable, hydrophobic dendronized **SPIO-G*n*-M** microspheres.

However, template-bound imines may possess remarkable stabilities in water (10) and require relatively large amounts of water (11) or demetallization in order to be dissociated into their corresponding amine and carbonyl components. Control over the substrate/product ratios in the equilibrium by the amount of water may give fine-tuned configurations of the system with a desired ratio of materials, instead of the all-or-nothing (substrate or product) situation.

Herein, we describe the use of hydrophobic poly(aryl ether) dendrons (12) to peripherally functionalize hydrophilic amine-containing SPIO microspheres (**SPIO-NH$_2$**) in one step via imine formation (Scheme 1). The reversible formation of imine bonds in the absence/presence of water renders dynamic control of the hydrophilicity and hydrophobicity of the microspheres. However, the dynamic nature of the imine-containing dendronized SPIOs (**SPIO-G*n***) can be "fixed" by locking the reversible 2,6-diiminopyridyl moieties with metal cations (Zn^{2+}, Co^{2+}, and Ni^{2+}) to afford kinetically stable microspheres (**SPIO-G*n*-M**). The functionalized microspheres are easily separable by an externally applied magnetic field. Because the **SPIO-G*n*** structures are subjected to hydrolysis, the dynamic wettabilities using different solvent systems as well as the contact-angle hystereses were explored.

RESULTS AND DISCUSSION

To begin with, the amine-functional, silica-coated Fe$_3$O$_4$ microspheres with an average diameter of 300 ± 30 nm (**SPIO-NH$_2$**) and the AB$_2$-type poly(aryl ether) dendron from the first generation (G1) to the third generation (G3) (12) were synthesized. The **SPIO-NH$_2$** microspheres were char-

acterized by transmission electron microscopy (TEM) and X-ray diffraction (XRD) spectroscopy (Figure S1 in the Supporting Information). TEM images reveal that the Fe$_3$O$_4$ microspheres that were synthesized (Figure 1a) using a solvothermal method possess a mean diameter of 220 ± 50 nm. Furthermore, a continuous layer, which exhibits (Figure 1b) a fine enhancement in brightness in comparison to the dark inner core, is clearly observed on the outer shell of the Fe$_3$O$_4$ cores. A typical single core/single shell nanostructure is observed, demonstrating the uniform morphology of the **SPIO-NH$_2$** microspheres bearing a silica layer with a thickness of ~80 nm. Moreover, there is no obvious change in the mean particle diameter of the Fe$_3$O$_4$ core after coating with silica, and the resulting **SPIO-NH$_2$** microspheres also possess a well-dispersed nature and spherical shape with an average diameter of 300 nm. The dendronized microspheres **SPIO-G*n*** also possess surface morphology similar to that of **SPIO-NH$_2$** under TEM. The organic dendron layers that are attached to the microspheres are relatively thin (<8 nm) (13), which cannot be clearly visualized and also cannot be differentiated from the silica layer under TEM.

The key step of the dendronization is the condensation reaction between the dendritic dialdehyde (**G*n*-CHO**) and the **SPIO-NH$_2$** microspheres. The multiple condensation reactions on the particles' surface are feasible via imine formation. Poly(aryl ether) dendrons (14) serve important roles in our structures; for example, they can (1) increase the solubility of the inorganic structures toward organic solvents, (2) reduce the self-aggregation between magnetic microspheres, and (3) expel any water molecules present in their hydrophobic dendritic microenvironments to give relatively stable
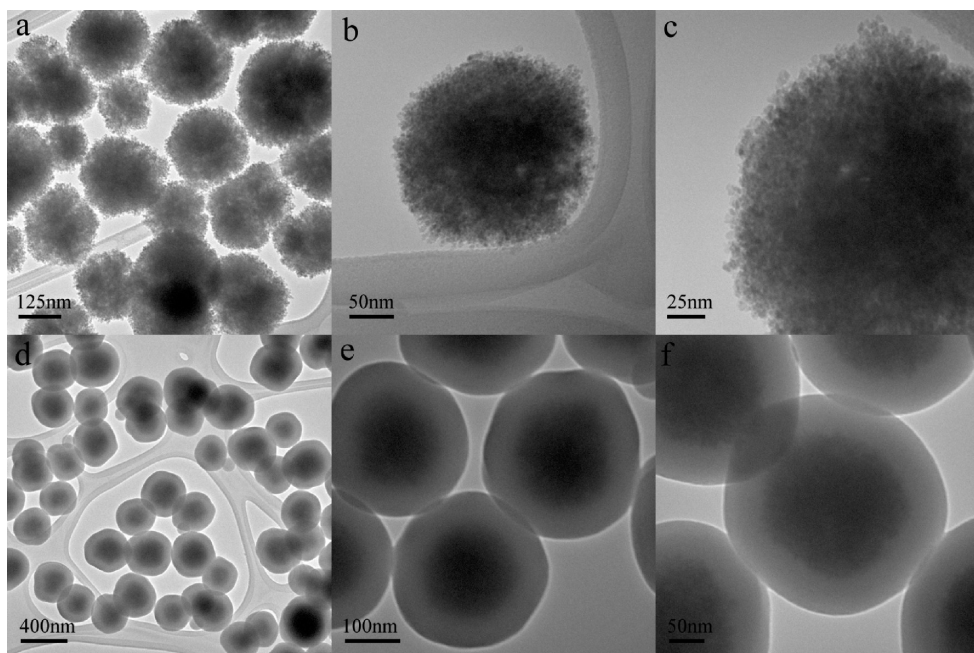
FIGURE 1. TEM images of (a−c) the Fe_3O_4 microspheres (average diameter = 220 ± 50 nm) and (d−f) the silica-coated Fe_3O_4 microspheres (SPIO-NH₂; average diameter = 300 ± 30 nm).

Dendrons incubated with SPIO-NH₂

Magnetic separation

Increasing [SPIO-NH₂]
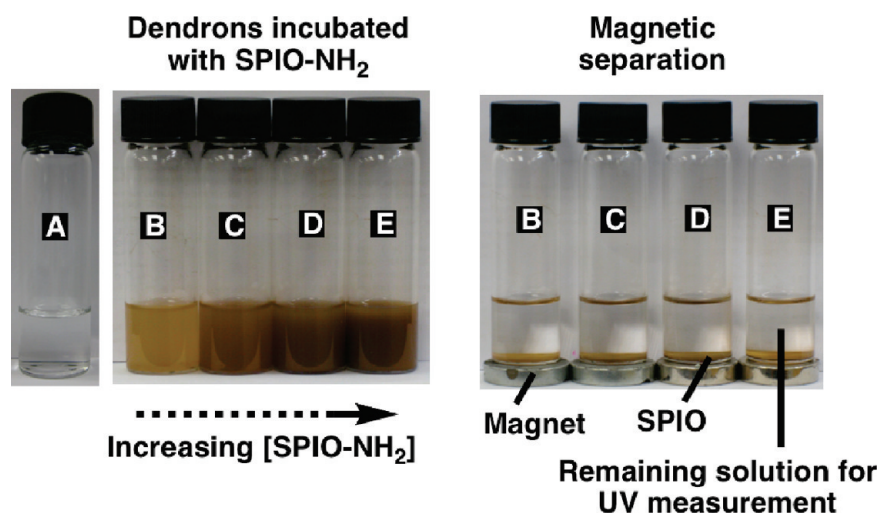
Magnet   SPIO

Remaining solution for UV measurement

FIGURE 2. Left: Pictures showing that the solutions of Gn-CHO dendron (1.15 mmol) were incubated with increasing amounts (mg) of the SPIO-NH₂ microspheres (A, 0; B, 0.5; C, 1.0; D, 3.0; E, 5.0) in MeCN/CH_2Cl_2 (3:1) to form the dispersed SPIO-Gn. Right: Incubated solutions were placed with four magnets at the bottom, leading to magnetic separation of SPIO-Gn at the bottom of the vials. The clear solutions were subsequently taken out for the UV/visible absorption spectroscopic measurements.

dendronized structures. The overall process simply requires the mixing and matching of microspheres and dendrons by equilibrating for at least 30 min. It has been found that the **SPIO-NH₂** microspheres are well-dispersed in MeOH or water, while the **SPIO-Gn** ($n = 1-3$) dendronized microspheres are well-dispersed in pure, less polar organic solvents such as $CHCl_3$, CH_2Cl_2, MeCN, PhMe, and tetrahydrofuran.

Because it could be a difficult task to measure the amounts of both microspheres and dendrons in exact stoichiometric ratios for the dendronization reactions, therefore, it is necessary to perform several titration experiments by mixing the two materials in different ratios. In these titration processes, the **SPIO-NH₂** microsphere is used as the limiting reagent, whereas a slight excess of dendrons is used.

After dendronization, excess dendrons can be washed away, whereas the resulting magnetic particles are attracted by an externally applied magnetic field.

Through a comparison of the consumptions of dendron and the efficiencies in forming the dendronized microspheres **SPIO-Gn** with imine bonds, a set of titration experiments was performed and then subsequently characterized by UV/visible absorption spectroscopy. First, solutions of **Gn-CHO** with a fixed concentration (1.15 mM) were incubated (Figure 2, left) with various amounts of **SPIO-NH₂** microspheres (0.5, 1.0, 3.0, and 5.0 mg) in MeCN/CH_2Cl_2 (3:1) to give **SPIO-Gn**. The color of the solution becomes darker and more turbid with increased concentrations of the **SPIO-NH₂** microspheres. After equilibration for 1 h, several neodymium−iron−boron magnets were placed at the bottom to
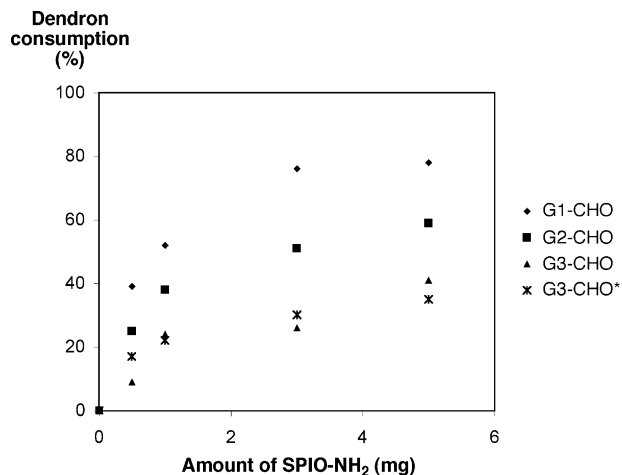
FIGURE 3. Plot of dendron consumption (%) versus the amounts of SPIO-NH$_2$ (mg) obtained from the UV/visible absorption spectroscopic results in MeCN/CH$_2$Cl$_2$ (3:1) with dendron concentrations of 1.15 or 57.5 mM.

FIGURE 4. FTIR spectra of (a) the as-prepared SPIO-NH$_2$ microspheres and (b) the SPIO-G3 microspheres.

attract magnetic particles (Figure 2, right) to the bottom of the vials. This operation leads to the magnetic separation of the particles within a minute. Subsequently, the resulting clear supernatant solutions were taken out such that the amount of remaining dendron in the solutions was analyzed by UV/visible absorption spectroscopy.

For the UV/visible spectroscopic traces of **G1-CHO** and **G3-CHO** dendrons, the absorption maxima (λ_{max}) for **G1-CHO** and **G3-CHO** dendrons are 224 and 227 nm, respectively. Generally, the stacked absorption spectra of the magnetically separated solutions show a decreasing signal intensity of the **G1-CHO** and **G3-CHO** dendrons after treatment of increasing amounts of the **SPIO-NH$_2$** microspheres (Figure S2 in the Supporting Information). For mixing between **G1-CHO** dendrons and **SPIO-NH$_2$** microspheres (1.15 mM), the consumption of **G1-CHO** dendrons almost reaches a plateau (78%) when 3−5 mg of the **SPIO-NH$_2$** microspheres was used (Figure 3). For the mixing of **G2-CHO** and **G3-CHO** separately with **SPIO-NH$_2$** microspheres (5 mg), the dendron consumptions are 59% and 41% (Figure 3), respectively. In the formation of **SPIO-Gn** dendronized microspheres, as a result, the dendron comsumptions decrease with an increase in the size of the dendrons from G1 to G3.

The difference in the percentage of dendron consumption in the condensation reactions accounts for the "dendritic effect" (15) from steric crowding; that is, less sterically hindered G1 dendrons can be incorporated onto the **SPIO** surface with a larger amount. This is because the **SPIO** particle's periphery is rough and contains nanofold, whereas a small perturbation in terms of the size of the dendron has a significant effect on the percentage of dendron attachment. Additionally, mixing between the **G3-CHO** dendron with various amounts of the **SPIO-NH$_2$** microspheres was performed at a concentration (57.7 mM) that was 20 times lower than that of the former experiments (1.15 mM). The percentage of G3 dendron consumption at low concentration is only slightly less effective (35% with 5 mg of **SPIO-NH$_2$** used), only a 6% decrease of dendron consumption in the solution. These observations clearly demonstrate the ef-
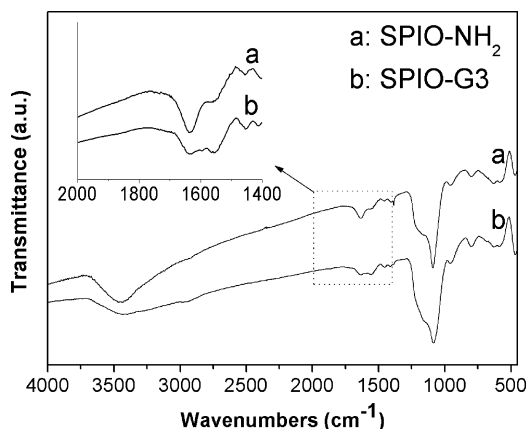
fectiveness of the imine-forming dendronization in the **SPIO-Gn** microsphere structures with maximum dendron occupancies. On the other hand, the **SPIO-Gn** microspheres are readily hydrolyzed in water-containing, wet organic solvents to give separate dendron and **SPIO-NH$_2$** components. UV/visible absorption spectroscopic analysis reveals that, in the presence of water, the dendrons on the **SPIO-Gn** microspheres could be released with the same amount that they had been previously attached onto the microspheres. Subsequently, the released dendrons could be reattached to the **SPIO-NH$_2$** microspheres once again by drying of the solvent system with anhydrous MgSO$_4$, Na$_2$SO$_4$, or molecules sieves (11).

In order to further confirm the successful attachment of dendrons onto the **SPIO-NH$_2$** microspheres, FTIR spectroscopy was employed. For instance, Figure 4a reveals the FTIR spectrum of the as-prepared **SPIO-NH$_2$** microspheres. The **SPIO-NH$_2$** microspheres have characteristic signals at ∼3450 (N−H stretching), 1650 (N−H bending), and 1100 (Si−O) cm^{-1}. On the other hand, Figure 4b reveals the FTIR spectrum of the **SPIO-G3** microspheres. The FTIR spectrum of the **SPIO-G3** microspheres possesses similar characteristic signals at ∼3450 (weak, N−H stretching), 1650 (N−H bending), and 1100 (Si−O) cm^{-1} but with new distinct signals at 1600 (C=N stretching) and 810 (trisubstituted aromatic ring) cm^{-1}. These observations reveal that the G3 dendrons were incorporated successfully onto the **SPIO-NH$_2$** microspheres via dynamic imine formation.

X-ray photoelectron spectroscopy (XPS) has been used for the surface characterization of various materials, and unambiguous results are readily obtained when each of the various surface components contains unique elemental markers. Here, XPS spectra were acquired (Figure S2 in the Supporting Information) for **SPIO-NH$_2$**, **SPIO-G3**, and **SPIO-G3-Zn**. All three structures give the signals of 532 eV (O 1s), 399 eV (N 1s), 284 eV (C 1s), and 102 eV (Si 2p). An additional peak at 1021 eV was also observed for the **SPIO-G3-Zn** structure, which corresponds to Zn 2p$_{3/2}$. The binding energy of 710 eV for Fe 2p was not observed in the spectra of the three structures, which further supports that all Fe$_3$O$_4$ cores in the microspheres are confined within a shell of silica, in agreement with the TEM results. The thermal
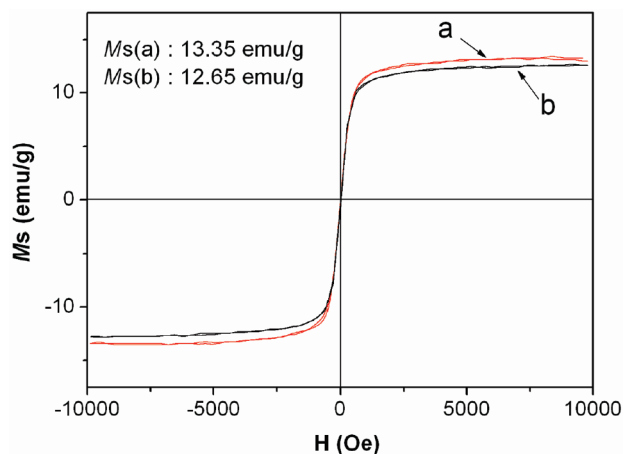
FIGURE 5. Hysteresis loops of (a) the as-prepared SPIO-G1 and (b) the SPIO-G3 microspheres.
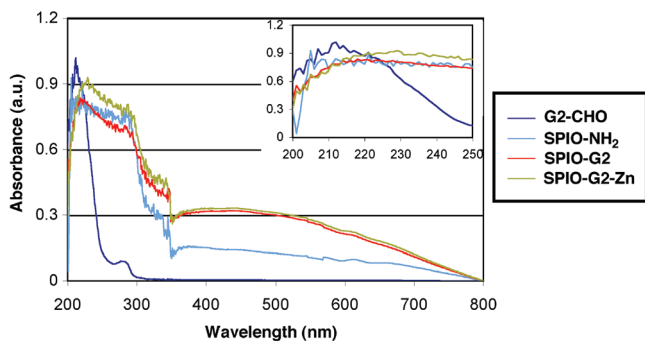

FIGURE 6. UV/visible absorption spectra of G2-CHO, SPIO-NH$_2$, SPIO-G2, and SPIO-G2-Zn microspheres in MeCN/MeOH (5:1; concentration ~0.5 mg/mL).
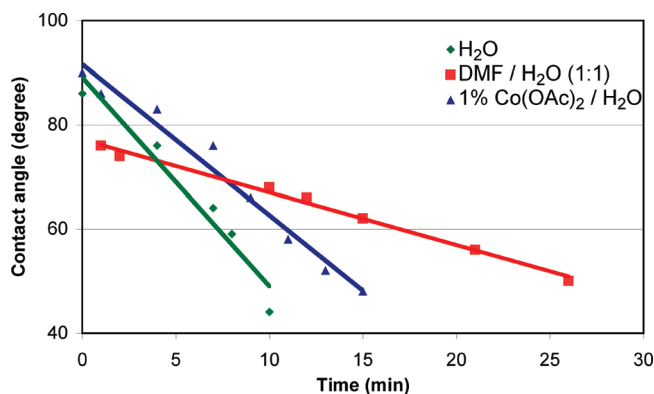

FIGURE 8. Plot of the contact angle (degree) versus time (min), showing the wettability of SPIO-G3 using a drop of H$_2$O, DMF/H$_2$O (1:1), or 1% Co(OAc)$_2$/H$_2$O.

stability of **SPIO-G3-Co** was characterized (Figure S3 in the Supporting Information) by thermogravimetric analysis (TGA). The result reveals a sharp mass loss of 22% at ~160 °C, which corresponds to a loss of the dendron. In the **SPIO-G3-Co** structure, therefore, there is 0.3 mg of dendron per mg of **SPIO** or 0.14 mmol of dendron per mg of **SPIO**.

The magnetic properties of the as-prepared dendronized microspheres **SPIO-Gn** were characterized by a vibrating sample magnetometer (VSM). Figure 5 reveals the hysteresis loops of the **SPIO-G1** (Figure 5a) and the **SPIO-G3** (Figure 5b) dendronized microspheres. The saturated magnetization (M_s) values were determined to be 13.35 emu/g for **SPIO-G1** and 12.65 emu/g for **SPIO-G3** microspheres at 298 K. No remanence was detected for the as-prepared product. The zero coercivity and the reversible hysteresis behavior indicate the superparamagnetic nature of the microspheres. Several factors, such as (1) the surface coverage of dendrons on **SPIO** particles, (2) the molecular weights of dendron and (3) the sizes of dendron, govern the M_s values. From the

evident that the **SPIO-Gn** microspheres have maximum dendron occupancies on the particles' surface, the effect of the resulting thickness of the dendritic layer on **SPIO** is dominant. In comparison to the **SPIO-G3** dendronized microspheres, therefore, the observation of a higher M_s value obtained for the **SPIO-G1** microspheres attributes to the thinner outer G1 dendritic layer (13).

Because of the multiple and readily hydrolyzable imine bonds, the three kinetically labile G1−G3 **SPIO-Gn** microspheres were treated in each case with a slight excess of metal salt [Zn(OAc)$_2$, Co(OAc)$_2$, or Ni(OAc)$_2$], to give the stable **SPIO-Gn-M** (M = Zn, Co, Ni) dendronized microspheres. Similarly, the metal-locked **SPIO-Gn-M** microspheres can also be well dispersed in common organic solvents. UV/visible absorption spectroscopy was employed for characterization of the as-prepared microspheres. After the **SPIO-Gn-M** microspheres were incubated with wet organic solvents and magnetically separated, the supernatant solutions were monitored by UV spectroscopy. The results reveal that there was approximately <5% detachment of dendrons. However, there was no detachment of dendrons when the **SPIO-Gn-M** microspheres were treated with pure water.

Figure 6 reveals the UV/visible absorption spectra of **G2-CHO**, **SPIO-NH$_2$**, **SPIO-G2**, and **SPIO-G2-Zn** microspheres in MeCN/MeOH (5:1). The absorption spectrum of the **SPIO-NH$_2$** microspheres shows a broad peak maximum plateau at 200−300 nm, then a gradual decrease in absorption at 300−350 nm, and then a decrease to 800 nm. The metal acetates show their UV absorptions from 200 to 260 nm (Figure S3A in the Supporting Information). By way of example, a set of the UV/visible absorption spectra involving G2 dendrons is compared (Figure 6) in MeCN/MeOH (5:1). The **G2-CHO** dendron demonstrates the maximum absorption (λ_{max}) at 213 nm, while the λ_{max} of the **SPIO-G2** micro-

FIGURE 7. Contact-angle measurement images of (left) SPIO-NH$_2$- and (right) SPIO-G2-Zn-coated mica surfaces.

Table 1. Contact-Angle Measurement Data (Solvent, Water; Measured 60 s after Deposition; Experimental Error ±2°)

structure	contact angle (deg)	structure	contact angle (deg)
SPIO-NH₂	42	**SPIO-G2-Zn**	85
SPIO-G1-Zn	83	**SPIO-G3-Zn**	86

Table 2. Contact-Angle Measurement Data of SPIO-G3 (Experimental Error ±2°)

	initial (deg)	final (deg)	hysteresis (deg)	rate (°/min)
H_2O	86	44	42	4.0
DMF/H_2O (1:1)	76	50	26	1.0
1 % $Co(OAc)_2/H_2O$	90	48	42	2.9

spheres is 215 nm. The absorption spectrum of **SPIO-G2** contains the characteristics of both **G2-CHO** and **SPIO-NH₂**. On the other hand, the UV/visible spectra of **SPIO-G2-Zn**, **SPIO-G2-Co**, and **SPIO-G2-Ni** are approximately identical, having a λ_{max} value of 230 nm (Figure S3B in the Supporting Information). Thus, it reveals a red shift ($\Delta\lambda = 15$ nm) in λ_{max} from the absorption spectrum of **SPIO-G2** (215 nm), leading to the conclusion that the metal complexes templated the formation of dendronized microspheres **SPIO-G2-M** most likely at the 2,6-diiminopyridyl moiety (6, 16).

The wettability of the as-prepared microspheres was analyzed using a contact-angle meter. In particular, the **SPIO-NH₂** microspheres demonstrate (Figure 7, left) a contact angle of $42 \pm 2°$ when a drop of water was added to the **SPIO-NH₂**-coated mica surface. Thus, this reveals that the **SPIO-NH₂** microspheres are relatively hydrophilic. On the other hand, the **SPIO-G2-Zn** dendronized microspheres demonstrate (Figure 7, right) a contact angle of $85 \pm 2°$ when a drop of water was added to the **SPIO-G2-Zn**-coated mica surface. This observation shows that the **SPIO-G2-Zn** dendronized microspheres are relatively hydrophobic and possess an increase of the contact angle over 40°. The **SPIO-G1-Zn** and **SPIO-G3-Zn** dendronized microspheres possess contact angles similar to that of **SPIO-G2-Zn** but with a slight increase of their contact angles with increasing dendron size (generation). Clearly, the dendronization of the particles results in a significant change of their hydrophobicities.

Furthermore, the slow dissociation of the dynamic **SPIO-Gn** dendronized micropsheres can be witnessed by contact-angle measurements. When a drop of water was placed on a **SPIO-Gn**-coated mica surface, the contact angle of the water droplet decreased in time (Figure S7 in the Supporting Information). This dynamic wettability of the **SPIO-Gn** structure was further exploited by using a relatively less polar solvent system, N,N'-dimethylformamide (DMF)/H_2O (1:1), as well as a Co^{2+} transition-metal-cation-containing aqueous solution, 1 % $Co(OAc)_2/H_2O$. Comparatively, the rate of decrease of the contact angle for **SPIO-G3** is $H_2O >$ 1 % $Co(OAc)_2/H_2O > DMF/H_2O$ (1:1) (Figure 8 and Table 2), with rates of 4.0, 2.9, and 1.0°/min, respectively. In particular, the use of a drop of 1 % $Co(OAc)_2/H_2O$ in the contact-angle measurement for **SPIO-G3** gives a lower rate of decrease in the contact angle. This observation could be due to the

temporary templating process between the imine groups of **SPIO-G3** and the Co^{2+} cations, which slows down the dissociation/hydrolysis process. A small amount of **SPIO-G3-Co** may exist as a product in the equilibrium, revealing a larger final contact-angle value (48°) compared to the value using H_2O (44°). On the other hand, the use of relatively less polar solvent system, DMF/H_2O (1:1), successfully reduces the dissociation rate of **SPIO-G3** toward hydrolysis, with a 1.0°/min decrease of the contact angle.

CONCLUSION

In conclusion, hydrophilic microspheres **SPIO-NH₂** have been converted into hydrophobic microspheres **SPIO-Gn** by one-step dendronization. Such a conversion is reversible and depends on the amount of water presented in the systems. However, the dynamic nature of the **SPIO-Gn** dendronized micropsheres can be "fixed" by a supramolecular metal ion templation to give the kinetically stable **SPIO-Gn-M** dendronized microspheres. Isolation of these microspheres is facilitated by convenient magnetic separation by an externally applied magnetic field. Characterization of these novel organic−inorganic hybrid microspheres was performed by using various techniques using UV/visible absorption and FTIR spectroscopies, TEM, and a VSM. We have demonstrated the stability, reversible switching of hydrophilicity/hydrophobicity, and magnetic separability of these materials. The dynamic wettabilty of the **SPIO-Gn** structures has been explored using three different solvent systems. Eventually, the catalytic properties of these materials, which are able to be operated in various common organic solvent systems and show recyclability, could be explored. By slight modifications of the different reactive metal species, the dendronized microspheres or nanoparticles can be potentially used as magnetic-separable, reusable catalysts for olefin polymerization and for other reactions using different supported noble metal cations (17). By combination of the advantageous abilities such as magnetic separation, dynamic reversibility, and increased solubility of dendritic (18) fragments toward organic solvents, it is feasible to reversibly modify the hydrophilic amine flat surface or other surfaces to a hydrophobic surface by versatile dynamic dendronization.

EXPERIMENTAL SECTION

Materials and Methods. The G1−G3 dendritic dialdehydes were synthesized according to a literature procedure (11). Ferric chloride hexahydrate ($FeCl_3 \cdot 6H_2O$), sodium acrylate (CH_2=CHCOONa), ethylene glycol ($C_2H_6O_2$), tetraethyl orthosilicate (TEOS; 98 %), (3-aminopropyl)triethoxysilane (APTES), absolute ethanol (EtOH; 95 wt %), and an aqueous ammonia solution (28 %) were purchased from Sigma-Aldrich. All chemicals were of analytical grade and used without further purification. Doubly deionized water was used throughout all of the processes. Powder XRD patterns of the products were obtained on a Japan Rigaku DMax-γA rotation-anode X-ray diffractometer equipped with graphite-monochromatized Cu Kα radiation ($\lambda = 1.541\ 78$ Å). TEM analysis was performed by using a FEI TecnaiF20 field-emission transmission electron microscope. IR spectra were recorded in the wavenumber range from 4000 to 500 cm^{-1} with a Nicolet model 759 FTIR spectrometer using a

KBr wafer. UV/visible absorption spectra were obtained using a Cary 5G UV/visible/NIR spectrophotometer with a scan rate of 600 nm/min. Measurements were performed twice. TGA was performed on a TA Instruments Hi-Res TGA 2950 thermogravimetric analyzer from 30 to 800 °C (heating rate = 50 °C/min). The magnetic properties ($M-H$ curve) were measured at room temperature on a Lakeshore 7300 magnetometer. Contact angles were measured using a Tantec CAM-MICRO contact-angle meter at ambient temperature with mica surfaces. The samples were drop-cast on a freshly cleaved mica surface at a concentration of ~0.5 mg/mL in MeCN/CH$_2$Cl$_2$ (3:1).

Synthesis of Fe$_3$O$_4$ Microspheres. The magnetic Fe$_3$O$_4$ particles were prepared through a solvothermal reaction. Briefly, FeCl$_3$·6H$_2$O (0.54 g) and sodium acrylate (1.5 g) were dissolved in ethylene glycol (20 mL) under magnetic stirring. The obtained homogeneous yellow solution was transferred to a Teflon-lined stainless-steel autoclave and sealed to heat at 200 °C. After reaction for 8 h, the autoclave was cooled to room temperature. The obtained magnetite particles were washed with EtOH and water several times and then dried in a vacuum for 12 h.

Synthesis of SPIO-NH$_2$ Microspheres. This process was performed via a sol−gel approach (19). In a typical procedure, the as-prepared magnetic sphere (25 mg) was mixed with water (3 mL) and EtOH (20 mL). The mixture was homogenized by ultrasonication for 30 min prior to the addition of an ammonia solution (1 mL). After that, a mixture of TEOS/EtOH (0.2 mL/5 mL) was injected into the solution over 30 min. After 1 h, APTES in EtOH (1.5 mL, 30 μL/5 mL, v/v) was added into the reaction solution over 20 min. Subsequently, the products were collected with the help of a magnet and washed with EtOH and water several times. Finally, the product was dried in a vacuum for 12 h to obtain the **SPIO-NH$_2$** core/shell microspheres.

Synthesis of SPIO-Gn Microspheres ($n = 1-3$). A mixture was prepared by mixing the **Gn-CHO** dendrons (1.15 mM) and **SPIO-NH$_2$** (1 mg/mL) in MeCN/CH$_2$Cl$_2$ (3:1). The mixture was shaken at room temperature for 24 h. The products were collected with the help of a magnet and washed with the solvent system MeCN/CH$_2$Cl$_2$ (3:1, 2 mL) twice. Finally, the product was dried in a vacuum for 12 h to obtain **SPIO-Gn** microspheres. For a typical example, **G3-CHO** (25 mg), **SPIO-NH$_2$** (10 mg), and MeCN/CH$_2$Cl$_2$ (3:1, 10 mL) were mixed to give the resulting **SPIO-G3** dendronized microspheres.

Synthesis of SPIO-Gn-M Microspheres ($n = 1-3$; M = Zn, Co, Ni). Method A. A mixture of the as-prepared **SPIO-Gn** dendronized microspheres (1 mg) was mixed with M(OAc)$_2$ (1.1 mM) in MeCN/MeOH (5:1). The mixture was shaken at room temperature for 24 h. The products were collected with the help of a magnet and washed with the solvent system MeCN/MeOH (5:1, 2 mL) twice. Finally, the product was dried in a vacuum for 12 h to obtain the **SPIO-Gn-M** microspheres. For a typical example, **SPIO-G2** (1 mg) and Zn(OAc)$_2$ (550 mg) were mixed in MeCN/MeOH (5:1, 3 mL) to give the resulting **SPIO-G2-Zn** microspheres.

Method B. A mixture was prepared by mixing the **Gn-CHO** dendrons (1 equiv), M(OAc)$_2$ (1 equiv), and **SPIO-NH$_2$** (1.2 mg/mmol) in MeCN/MeOH (5:1). The mixture was shaken at room temperature for 24 h. The products were collected with the help of a magnet and washed with the solvent system MeCN/MeOH (5:1, 2 mL) twice. Finally, the product was dried in a vacuum for 12 h to obtain the **SPIO-Gn-M** microspheres. For a typical example, **G2-CHO** (9.2 mg), Zn(OAc)$_2$ (1.5 mg), **SPIO-NH$_2$** (10 mg), and MeCN/MeOH (5:1, 3 mL) were mixed to give the resulting **SPIO-G2-Zn** microspheres.

Note Added after ASAP Publication. This paper was published ASAP on August 28, 2009 with a misspelling in Figure 2 and a minor text error. The corrected version was published ASAP on September 8, 2009.

Supporting Information Available: XRD, XPS, TGA, and UV/visible absorption spectroscopic and contact-angle characterization data. This material is available free of charge via the Internet at http://pubs.acs.org.

REFERENCES AND NOTES

(1) (a) Descalzo, A. B.; Martínez-Máñez, R.; Sancenón, F.; Hoffmann, K.; Rurack, K. *Angew. Chem., Int. Ed.* **2006**, *45*, 5924–5948. (b) Saha, S.; Leung, K. C.-F.; Nguyen, T. D.; Stoddart, J. F.; Zink, J. I. *Adv. Funct. Mater.* **2007**, *17*, 685–693.

(2) (a) Nijhuis, C. A.; Ravoo, B. J.; Huskens, J.; Reinhoudt, D. N. *Coord. Chem. Rev.* **2007**, *251*, 1761–1780. (b) Leung, K. C.-F.; Chak, C.-P.; Lo, C.-M.; Wong, W.-Y.; Xuan, S. H.; Cheng, C. H. K. *Chem. Asian J.* **2009**, *4*, 364–381.

(3) (a) Berná, J.; Leigh, D. A.; Lubomska, M.; Mendoza, S. M.; Pérez, E. M.; Rudolf, P.; Teobaldi, G.; Zerbetto, F. *Nat. Mater.* **2005**, *4*, 704–710. (b) Chang, T.; Rozkiewicz, D. I.; Ravoo, B. J.; Meijer, E. W.; Reinhoudt, D. N. *Nano Lett.* **2007**, *7*, 978–980. (c) Rizzello, L.; Shankar, S. S.; Fragouli, D.; Athanassiou, A.; Cingolani, R.; Pompa, P. P. *Langmuir* **2009**, *25*, 6019–6023.

(4) Laurent, S.; Forge, D.; Port, M.; Roch, A.; Robic, C.; Elst, L. V.; Muller, R. N. *Chem. Rev.* **2008**, *108*, 2064–2110.

(5) Meyer, C. D.; Joiner, C. S.; Stoddart, J. F. *Chem. Soc. Rev.* **2007**, *36*, 1705–1723.

(6) (a) Chichak, K. S.; Cantrill, S. J.; Pease, A. R.; Chiu, S.-H.; Cave, G. W. V.; Atwood, J. L.; Stoddart, J. F. *Science* **2004**, *304*, 1308–1312. (b) Cantrill, S. J.; Chichak, K. S.; Peters, A. J.; Stoddart, J. F. *Acc. Chem. Res.* **2005**, *38*, 1–9.

(7) Pentecost, C. D.; Chichak, K. S.; Peters, A. J.; Cave, G. W. V.; Cantrill, S. J.; Stoddart, J. F. *Angew. Chem., Int. Ed.* **2007**, *46*, 218–222.

(8) Liu, X.; Liu, Y.; Li, G.; Warmuth, R. *Angew. Chem., Int. Ed.* **2006**, *45*, 901–904.

(9) Rowan, S. J.; Cantrill, S. J.; Cousins, G. R. L.; Sanders, J. K. M.; Stoddart, J. F. *Angew. Chem., Int. Ed.* **2002**, *41*, 898–952.

(10) Saggiomo, V.; Lüning, U. *Eur. J. Org. Chem.* **2008**, 4329–4333.

(11) Dissociation of an ammonium-templated, imine-containing dynamic [2]rotaxane in H$_2$O/MeCN was investigated (unpublished results). Large amounts of H$_2$O (>100 equiv) are required for the dissociation of 52 % of [2]rotaxanes. The dissociated components are relatively stable in the presence of large amounts of water and can also be reassembled to afford the dynamic [2]rotaxanes once again by eliminating water from the aqueous solutions in the presence of various drying agents (unpublished results). For the structural formula of ammonium-templated, imine-containing dynamic [2]rotaxane, see: Glink, P. T.; Oliva, A. I.; Stoddart, J. F.; White, A. J. P.; Williams, D. J. *Angew. Chem., Int. Ed.* **2001**, *40*, 1870–1875.

(12) (a) Leung, K. C.-F.; Aricó, F.; Cantrill, S. J.; Stoddart, J. F. *J. Am. Chem. Soc.* **2005**, *127*, 5808–5810. (b) Leung, K. C.-F.; Aricó, F.; Cantrill, S. J.; Stoddart, J. F. *Macromolecules* **2007**, *40*, 3951–3959. (c) Leung, K. C.-F. *Macromol. Theory Simul.* **2009**, *18*, 328–335.

(13) Leung, K. C.-F.; Mendes, P. M.; Magonov, S. N.; Northrop, B. H.; Kim, S.; Patel, K.; Flood, A. H.; Tseng, H.-R.; Stoddart, J. F. *J. Am. Chem. Soc.* **2006**, *128*, 10707–10715.

(14) Chow, H.-F.; Leung, C.-F.; Wang, G.-X.; Zhang, J. *Top. Curr. Chem.* **2001**, *217*, 1–50.

(15) Helms, B.; Fréchet, J. M. J. *Adv. Synth. Catal.* **2006**, *348*, 1125–1148.

(16) Control experiments were performed (Figure S6 in the Supporting Information) by comparing the UV/visible absorption spectra of two complexes: (1) **G2-CHO** condensed with *n*-butylamine and (2) **G2-CHO** condensed with *n*-butylamine and Ni(OAc)$_2$. A red shift ($\Delta\lambda \sim 10$ nm) in λ_{max} is also observed from the complex (1)

to the metalated complex (2) in MeCN/MeOH (5:1). For UV/visible measurements with scan rates of 300 and 100 nm/min, the data points fluctuate because of the scattering of particles.

(17) (a) Gupta, K. C.; Sutar, A. K. *Coord. Chem. Rev.* **2008**, *252*, 1420–1450. (b) Kim, I.; Ha, Y. S.; Ha, C.-S. *Macromol. Rapid Commun.* **2004**, *25*, 1069–1072. (c) Miller, K. J.; Kitagawa, T. T.; Abu-Omar, M. M. *Organometallics* **2001**, *20*, 4403–4412. (d) Hutchings, G. J.; Brust, M.; Schmidbaur, H. *Chem. Soc. Rev.* **2008**, *37*, 1759–1765.

(18) (a) Astruc, D.; Chardac, F. *Chem. Rev.* **2001**, *101*, 2991–3024. (b) Liu, H.; Guo, J.; Jin, L.; Yang, W.; Wang, C. *J. Phys. Chem. B* **2008**, *112*, 3315–3321. (c) Jiang, Y.; Jiang, J.; Gao, Q.; Ruan, M.; Yu, H.; Qi, L. *Nanotechnology* **2008**, *19*, 075714.

(19) Ge, J. P.; Hu, Y. X.; Zhang, T. R.; Yin, Y. D. *J. Am. Chem. Soc.* **2008**, *129*, 8974–8975.

AM900367A